A Statistical Temperature Emissivity Separation Algorithm for Hyperspectral System Modeling

Runchen Zhao, Emmett J. Ientilucci, *Senior Member, IEEE*, and Peter Bajorski, *Senior Member, IEEE*

***Abstract*— With the popular use of remote sensing techniques, investigations into hyperspectral system designs and parameter trade-off studies have become more and more necessary. Analytical models based on statistical descriptions and energy propagation are certainly efficient methods to examine a large number of parameter trades and sensitive studies with low computational cost. In long wave Infrared (LWIR), an analytical version of a temperature/emissivity separation (TES) algorithm can be used to retrieve ground emissivity statistics. However, such a statistical analytical algorithm has not been fully developed, as far as we know. In this letter, a new statistical iterative spectrally smooth temperature/emissivity separation (S-ISSTES) algorithmic approach is proposed. The derivation and comparison of our statistical approach is discussed in detail. We show that it can retrieve first- and second-order statistics of surface spectra as well as the associated temperature from at-sensor radiance data. Experimental results using both real and synthetic data demonstrate the effectiveness of the proposed S-ISSTES algorithm.**

***Index Terms*— Forecasting and analysis of spectroradiometric system performance (FASSP), hyperspectral, long wave Infrared (LWIR), remote sensing, statistical iterative spectrally smooth temperature/emissivity separation (S-ISSTES), statistical modeling, temperature/emissivity separation (TES).**

I. Introduction

OVER the years, remote sensing and remote sensing systems have been used in a variety of fields and applications ranging from precision agriculture and biomass estimation to spectral unmixing and target detection. In the latter cases of unmixng and target detection, we often work in a reflectance space where the effects of atmosphere have been removed. The removal of atmospheric effects, or atmospheric compensation, has been the subject of research for decades and varies depending on whether one is working with data collected in VNIR/SWIR or long wave Infrared (LWIR). In the latter case, we need to concern ourselves with the estimation or separation of both ground-leaving emissivty and temperature, which is the domain we will be investigating in this letter.

Nevertheless, system modeling has become a commonly used tool for both the prediction of system performance and the analysis of system trades. Detailed first-principles physics-based simulations can take a well-defined scene and predict the sensor reaching radiance. This approach can create a dataset for algorithmic development and provide a phenomenological basis for explaining imagery collected by a real sensor [1]. However, this type of simulation usually has a high computational cost and can be very time-consuming during data preparation. An alternative approach is to use a statistical description of the scene and sensor and then forward propagate this information using analytical equations to predict system performance. That is precisely what the forecasting and analysis of spectroradiometric system performance (FASSP) model does [1]–[3], for example. This analytical approach reduces computation cost and complexity enabling a large number of efficient parameter trade-off and sensitivity studies.

Thus, the objective of this letter is to introduce a new statistical temperature/emissivity separation (TES) algorithm based on the propagation of first- and second-order statistics to support analytical simulations and system performance studies. This compact module, to be called statistical iterative spectrally smooth temperature/emissivity separation (S-ISSTES), can be plugged into any analytical performance model such as the one mentioned above (i.e., FASSP) or used standalone for target detection studies or any study that requires emissivity distributions or statistics. In this letter, we illustrate the module, its derivation, and comparison of its operation with synthetic and real hyperspectral imagery. Thus, this letter is outlined as follows: In Section II-A, we introduce a TES algorithm followed by a detailed derivation of our new S-ISSTES algorithm in Section II-B. In Section III, we illustrate two comparison studies using both real and synthetic data. We found that first- and second-order emissivity statistics as well as temperature were accurately retrieved using the new S-ISSTES algorithm.

II. Methodology

A. ISSTES

The iterative spectrally smooth temperature/emissivity separation (ISSTES) algorithm was originally proposed by Borel [4] and [5]. ISSTES uses atmospheric radiance data as its input and a smoothness assumption about the retrieved emissivity, which is really an evaluation criterion about the output results. In describing this algorithm, we first start with a model of the at-sensor radiance in the LWIR. That is,

$$L_t = L_D(1-\varepsilon_t)\tau + L_B(T_t)\varepsilon_t\tau + L_U \tag{1}$$

Manuscript received May 24, 2021; revised October 4, 2021; accepted December 9, 2021. Date of publication January 6, 2022; date of current version January 27, 2022. *(Corresponding author: Runchen Zhao.)*

Runchen Zhao and Emmett J. Ientilucci are with the Digital Imaging and Remote Sensing Laboratory, Chester F. Carlson Center for Imaging Science, Rochester Institute of Technology, Rochester, NY 14623 USA (e-mail: rxz1973@rit.edu; emmett@cis.rit.edu).

Peter Bajorski is with the School of Mathematical Sciences, College of Science, Rochester Institute of Technology, Rochester, NY 14623 USA (e-mail: pxbeqa@rit.edu).

Digital Object Identifier 10.1109/LGRS.2022.3140754

where the subscript t represents the "target," L_t is the at-sensor radiance of the target, L_D represents the downwelling radiance, ε_t is the target emissivity, $L_B(T_t)$ is the blackbody radiance at the given temperature T_t, L_U is the upwelling radiance, and τ is the atmospheric transmittance.

To use ISSTES, the at-sensor radiance of a ground-truth panel or a graybody object with high emissivity (e.g., a "typical" emissivity with a spectrally flat value equal to 0.95 [6]) needs to be calculated using (1), and then the surface-leaving radiance, L_{surf}, can be obtained if the atmospheric profile is known. The unknown temperature T_0 can be estimated by

$$T_0 = \frac{1}{\lambda_1 - \lambda_2} \int_{\lambda_1}^{\lambda_2} L_B^{-1}(L_{\text{surf}}(\lambda), \lambda) d\lambda \tag{2}$$

where λ_1 and λ_2 define an atmospheric window. This estimated ground-truth temperature is treated as a reference temperature. Thus, by bracketing and extending the reference temperatures (i.e., $T_0 \pm 1$ K, ± 2 K, etc.), one can construct n number of retrieved target temperature candidates, $\hat{T}_{t,n}$. This extension can be any size as long as the range can cover the potential retrieved result. Third, rearranging the forward equation of (1), a series of retrieved target spectral emissivity candidates $\hat{\varepsilon}(\hat{T}_{t,n})$, for a single band i, can be computed as a function of their corresponding at-sensor radiances and temperature candidates. That is,

$$\hat{\varepsilon}_i(\hat{T}_{t,n}) = \frac{L_t(\epsilon_t, T_t)_i - (L_U)_i - (L_D\tau)_i}{\left(L_B\left(\hat{T}_{t,n}\right)\tau\right)_i - (L_D\tau)_i} \tag{3}$$

where again ϵ_t is the mean surface emissivity of the target and T_t is the corresponding target's temperature. The selection process is based on the assumption that a real surface emissivity spectrum has a smoother shape than the spectral features caused by atmospheric effects. Finally, a standard criterion called the "smoothness of the retrieved emissivity" is defined as

$$S_n = \sum_{i=2}^{k-1} \left(\hat{\varepsilon}_{i,t} - \frac{\hat{\varepsilon}_{i-1,t} + \hat{\varepsilon}_{i,t} + \hat{\varepsilon}_{i+1,t}}{3} \right)^2 \tag{4}$$

where i stands for the band center. This gives us the smoothness at a particular retrieved temperature candidate n. This is followed by the computation of the first-order derivative of the spectral smoothness, which is

$$\text{Derivative} = \frac{S_n - S_{n-1}}{\hat{T}_{t,n} - \hat{T}_{t,n-1}}. \tag{5}$$

The correct emissivity should be the smoothest curve among all the candidates. The corresponding temperature would be the estimate of the target's surface temperature.

B. Derivation of S-ISSTES

In Section II-A, we discussed how the ISSTES algorithm works. In this section, a new derivation illustrating the second-order transformation of statistics based on the ISSTES algorithm will be shown.

We need to first calculate the variance of the retrieved emissivity, $\hat{\varepsilon}_i(\hat{T}_{t,n})$. This is accomplished by calculating the variance of (3). T_t and ε_t are treated as random variables such that the variance can be expressed as

$$\text{Var}(\hat{\varepsilon}_i(\hat{T}_{t,n})) = \text{Var}\left(\frac{L_t(\epsilon_t, T_t)_i - (L_U)_i - (L_D\tau)_i}{\left(L_B\left(\hat{T}_{t,n}\right)\tau\right)_i - (L_D\tau)_i} \right). \tag{6}$$

In the denominator, we note that the retrieved temperature candidates $\hat{T}_{t,n}$ should also be treated as a random variable. For simplicity at this point, we will leave the denominator notation unchanged. One way to solve (6) is to break up the expression into two parts. We will use X to represent the numerator and Y to represent one over denominator. Thus, the variance of $\hat{\varepsilon}_i(\hat{T}_{t,n})$ can be rewritten cleanly as

$$\text{Var}\left(\hat{\varepsilon}_i\left(\hat{T}_{t,n}\right)\right) = \text{Var}(XY). \tag{7}$$

At this point, a brief discussion related to the dependency of X and Y is warranted. The random variable in the quantity X is the at-sensor radiance which contains uncertainties from the target surface emissivity, the surface temperature, atmospheric effects, and sensor noise. The uncertainties in Y are mainly from the random variable, $\hat{T}_{t,n}$. This retrieved temperature is estimated from the ground-truth panel surface temperature. Therefore, it is a reasonable assumption to assume that X and Y are independent of each other. Thus, (7) can be written as

$$\text{Var}(XY) = \text{Var}(X)\,\text{Var}(Y) + \text{Var}(X)[\text{E}(Y)]^2 + \text{Var}(Y)[\text{E}(X)]^2. \tag{8}$$

That is, $\text{E}(X)$, $\text{Var}(X)$, $\text{E}(Y)$, and $\text{Var}(Y)$ can be calculated, respectively. $\text{E}(X)$ can be written as

$$\text{E}(X_i) = L_t(\epsilon_t, T_t)_i - (L_U)_i - (L_D\tau)_i. \tag{9}$$

Considering L_U and $L_D\tau$ are not functions of random variables T_t, ϵ_t, and $\hat{T}_{t,n}$, they can be treated as constants. Thus, the variance of X only depends on the variance of the at-sensor radiance. Therefore, $\text{Var}(X)$ for each band center can be written as

$$\begin{aligned} \text{Var}(X_i) &= \text{Var}(L_t(\epsilon_t, T_t)_i - (L_U)_i - (L_D\tau)_i) \\ &= \text{Var}(L_t(\epsilon_t, T_t)_i) \end{aligned} \tag{10}$$

where $\text{Var}(L_t(\epsilon_t, T_t))$ can be known. This can be determined from multiple measurements or computed using the forward equation discussed in Appendix A. Similarly, the expectation of Y can be written as

$$\text{E}(Y_i) = \text{E}\left(\frac{1}{\left(L_B\left(\hat{T}_{t,n}\right)\tau\right)_i - (L_D\tau)_i} \right). \tag{11}$$

Again, L_D and τ can be treated as constants. Thus, the variance of Y can be defined as

$$\text{Var}(Y_i) = \text{Var}\left(\frac{1}{\left(L_B\left(\hat{T}_{t,n}\right)\tau\right)_i - (L_D\tau)_i} \right). \tag{12}$$

Finally, using (6) by rewriting (7) and additional details in deriving the variance of Y, found in Appendix B, the resulting

retrieved emissivity variance $\mathrm{Var}(\hat{\varepsilon}_i(\hat{T}_{t,n}))$ is

$$\begin{aligned}\mathrm{Var}(\hat{\varepsilon}_i(\hat{T}_{t,n})) &= \sigma_{\hat{T}}^2\left(\frac{dL_B}{d\hat{T}}\right)^2\frac{1}{\tau^2}\frac{1}{\left(L_B-L_D\right)^4}\mathrm{Var}(L_t(\epsilon_t,T_t)_i)\\ &\quad+\mathrm{Var}(L_t(\epsilon_t,T_t)_i)\,\mathrm{E}\left(\frac{1}{\left(L_B\left(\hat{T}_{t,n}\right)\tau\right)_i-(L_D\tau)_i}\right)\\ &\quad+\sigma_{\hat{T}}^2\left(\frac{dL_B}{d\hat{T}}\right)^2\frac{1}{\tau^2}\frac{1}{\left(L_B-L_D\right)^4}\\ &\quad\times\left[L_t\left(\overline{\epsilon}_t,\overline{T}_t\right)_i-(L_U)_i-(L_D\tau)_i\right]^2. \end{aligned}\tag{13}$$

After obtaining the variance $\mathrm{Var}(XY)$, the multivariate version (i.e., covariance) can be expressed as

$$\Sigma_{XY}=\Lambda_{\sigma Y}\Sigma_X\Lambda_{\sigma Y}+\Lambda_{\overline{Y}}\Sigma_X\Lambda_{\overline{Y}}+\Lambda_{\overline{X}}\Sigma_Y\Lambda_{\overline{X}}\tag{14}$$

where $\Lambda_{\sigma Y}$ is a diagonal matrix of standard deviations from $1/\tau L_B-\tau L_D$ and Σ_X is the full-spectral covariance matrix of $L_t-L_U-\tau L_D$, which is similar to that shown in (19). $\Lambda_{\overline{Y}}$ is the diagonal matrix of $\overline{Y}$, $\Lambda_{\overline{X}}$ is the diagonal matrix of $\overline{X}$, and Σ_Y is the spectral covariance of $1/\tau L_B-\tau L_D$, which can be calculated by $\Lambda_{\sigma Y}[1]\Lambda_{\sigma Y}$ where [1] is a $k\times k$ matrix of ones. Σ_Y is a $k\times k$ diagonal matrix, and the non-zero elements have the same expression as shown in (12).

III. Comparison With Simulations and Real Data

To validate our algorithm, two experiments were implemented which compared ground-truth emissivity statistics with analytical retrieved emissivity statistics (i.e., S-ISSTES), for both the simulated radiance data and real measured radiance data as shown in Fig. 1.

Absolute percentage error was used as an evaluation metric. The error between the mean ground emissivity and mean retrieved emissivity was calculated as $\mathrm{Error}_\epsilon=\sum_{k=0}^{N}\|\overline{\epsilon}_k-\hat{\overline{\epsilon}}_k\|/\overline{\epsilon}_k M$ where $\overline{\epsilon}_k$ is the mean ground emissivity at spectral channel k, $\hat{\overline{\epsilon}}_k$ is the mean retrieved emissivity at the same spectral channel, and M is the total number of spectral channels. The error between the ground emissivity covariance and the analytically derived covariance was calculated as $\mathrm{Error}_c=\sum_{i,j=0}^{N}\|\Sigma_{i,j}-\hat{\Sigma}_{i,j}\|/\Sigma_{i,j}M$ where i,j indicates the location of the corresponding covariance matrix, $\Sigma_{i,j}$ is the emissivity covariance matrix obtained from ground emissivities, $\hat{\Sigma}_{i,j}$ is the retrieved emissivity covariance matrix from the analytical method, and N is the number of values in the matrix. $\mathrm{Error}_{\overline{T}}=\overline{T}-\hat{\overline{T}}$ where $\overline{T}$ is the mean ground temperature and $\hat{\overline{T}}$ is the mean retrieved temperature.

A. Experiment Using an Analytical System Model

To support hyperspectral system designs and parameter trade-off studies, a model, briefly mentioned in Section I, called FASSP has been developed. The FASSP model uses a forward statistical transformation model and a backward compensation model to simulate at-sensor radiance (how we used it in this experiment) and retrieved surface reflectance or emissivity. More specifically, the statistical description of surface spectra (either reflectance or emissivity) is propagated through atmosphere (including atmospheric effects) with the addition of sensor artifacts and noise so as to generate at-sensor radiance data. As a result, the performance of remote sensing systems, coupled with the behavior of input spectra, can be analyzed while taking into account uncertainties from various parts of the system (i.e., sensor noise, etc.), though no TES algorithm exists in the model until this research presented in this letter. Thus, the new S-ISSTES module will be used to expand the capability of the FASSP model (or any other model, for that matter) so as to obtain retrieved surface temperature and emissivity statistics in LWIR.

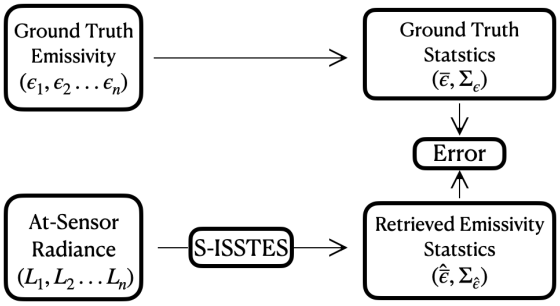

Fig. 1. Experimental approach comparing ground-truth emissivity statistics, $\overline{\epsilon}$, Σ_ϵ, with S-ISSTES-retrieved emissivity statistics, $\hat{\overline{\epsilon}}$, $\Sigma_{\hat{\epsilon}}$.

TABLE I
Errors Between Laboratory-Measured and Analytically Retrieved Data Based on Simulations

	Temperature Error [K]	Emissivity Error [%]	Covariance Error [%]
Material 1	0.0797	0.0083	0.7376
Material 2	0.0797	0.0027	0.7882
Material 3	0.0797	0.0023	0.6363

Three sets of laboratory LWIR-measured emissivity spectra (i.e., road and two vegetation materials, 600–4000 samples each) were used to evaluate the performance of our S-ISSTES implementation (upper left Fig. 1). For each set of data, the mean at-sensor radiance was directly estimated using FASSP and used as input to S-ISSTES as shown in the lower left of Fig. 1. In FASSP processing, the atmospheric conditions were defined using a 30 meteorological range (i.e., visibility), Mid-Latitude Summer atmospheric model, and Nadir sensor viewing, and all had a target surface temperature of 288.15 K. S-ISSTES was then used to retrieve temperature and emissivity from these three radiance datasets. The results can be seen in Table I including the differences in the laboratory measures and retrieved covariances as well as temperatures.

The errors shown in Table I are very low, as expected. This was more of a sanity check to confirm our implementation of S-ISSTES and (13). The errors are due to computational precision. In Section III-B, we examine S-ISSTES with real hyperspectral image data.

B. Experiment Using AHI Data

AHI sensor is a helicopter-borne LWIR hyperspectral imager which covers 7.5–11.5 μm with 256 spectral bands. To test S-ISSTES, we used AHI LWIR radiance data taken

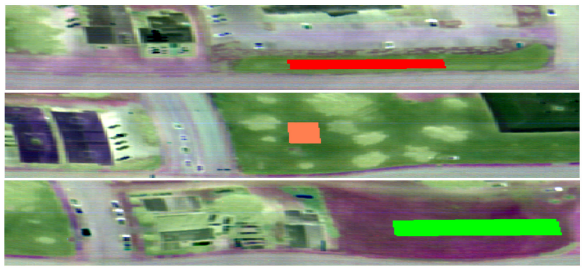

Fig. 2. False color AHI LWIR images were generated using bands 20, 96, and 176 (8, 9.3, and 10.7 μm). The overall mean and covariance were computed from various ROIs. ROI 1 is in green, ROI 2 is in orange, and ROI 3 is in red.

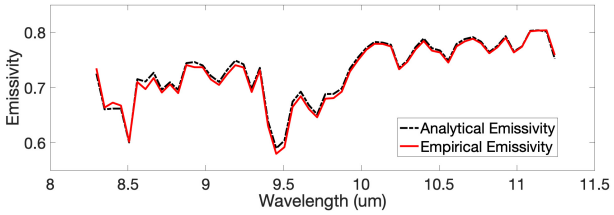

Fig. 3. Comparison of the analytically retrieved mean emissivity and ground-truth emissivity of ROI 1 (green) in Fig. 2.

over Yuma proving ground in Yuma, Arizona, on February 14, 2006. The observational data region(s) of interest (ROI) were carefully selected (i.e., considering region uniformity and avoiding image artifacts) at different locations in the data. Referring to Fig. 2, ROI 1 was selected from the green region (4455 pixels), ROI 2 from the orange region (2432 pixels), and ROI 3 from the red region (1610 pixels). For our study, 180 bands were selected from 256 bands and were then binned down to 60 bands so as to improve the signal-to-noise ratio (SNR). The atmospheric radiative code, Moderate Resolution Atmospheric Transmission (MODTRAN), was used to generate look-up tables (LUTs) for both downwelling and upwelling radiances as well as transmission.

Due to the lack of ground-truth emissivity in the AHI dataset, ISSTES was used to obtain reasonable "ground-truth" emissivity data (i.e., we applied ISSTES to each pixel in each ROI). This is reasonable considering the reported low error using ISSTES for emissivity retrieval (i.e., 0.002 error at 2-km altitude [7]). We then computed the "ground-truth" emissivity statistics (upper row Fig. 1). Our comparison experiment consisted of comparing "ground-truth" emissivity statistics with analytically retrieved emissivity statistics (i.e., using our S-ISSTES algorithm), for the three observational groups of LWIR data. To compute the analytical covariance, S-ISSTES was applied to the mean at-sensor radiance, $\overline{L}$ from each ROI. The temperature used to obtain the covariance was calculated as $\overline{T} = \sum_{n=0}^{N} T_n/N$ where T_n is the temperature of each pixel from the ISSTES method. The standard deviation of the temperature is an adjustable user-defined parameter, which can be iteratively examined in the comparison approach. A comparison between the retrieved mean emissivity and the mean ground emissivity of the green ROI in Fig. 2 can be seen in Fig. 3. A summary of these results can be seen in Table II.

TABLE II
ERROR BETWEEN EMPIRICALLY AND ANALYTICALLY OBTAINED DATA

	Temperature Mean/ Error $[K]$	Emissivity Error $[\%]$	Covariance Error $[\%]$
ROI 1	288/ 0.5	2.2	2.3
ROI 2	293/ 1.0	1.6	4.1
ROI 3	291/ 1.0	0.8	2.4

We can see that there are some minor differences between "ground-truth" emissivity statistics and analytically retrieved emissivity statistics. One of the main reasons for this is that for the analytical method, we made an assumption in (8) where the at-sensor radiance from the observed ROI was independent of the retrieved temperature of the ground truth. However, in the AHI data, the ground truth was not available. The retrieved temperature was calculated from the observed ROI. Another subtle difference is related to the fact that we calculated an average at-sensor radiance so as to create a mean radiance for the analytical approach. This is not necessarily an ideal way to create test cases since the area-averaged temperature of a region is not exactly the same as the temperature derived from the radiance averaged over the pixels footprint, even for blackbodies [8]. In light of these observational differences, which are really attributable to the fact that we are using real data, we can see that the S-ISSTES module performed as expected.

IV. CONCLUSION

This letter has introduced a new TES algorithm called S-ISSTES, which is based on the ISSTES algorithm. S-ISSTES retrieves emissivity statistics rather than single emissivity spectra, for example. This was developed by deriving what the transformation of statistics would be through the ISSTES algorithm. We then evaluated this algorithm using two experiments: 1) comparing measured ground-truth emissivity spectra (with computed statistics) with retrieved emissivity statistics from S-ISSTES (using FASSP to generate the at-sensor radiance used as input to S-ISSTES) and 2) comparing ISSTES-derived "ground-truth" emissivity (with computed statistics) with retrieved emissivity statistics from S-ISSTES (using actual AHI at-sensor radiance data). Both the experiments showed that S-ISSTES correctly retrieved first- and second-order emissivity statistics. Anyone performing LWIR modeling that needs emissivity statistics (e.g., as input to target detection models where target and background distributions are needed to generate receiver operating characteristic (ROC) curves) can use our new module. Future work will actually integrate the S-ISSTES module into our analytical FASSP model for system predictions in LWIR.

APPENDIX A
VARIANCE OF AT-SENSOR RADIANCE

Considering dominant full-spectrum sources of energy, we can express the at-sensor radiance of a target t as

$$L_t = L_D \rho \tau + L_B(T)[1-\rho]\tau + L_{\text{adj}}(\rho_{\text{adj}}) + L_U \quad (15)$$

where L_D represents the total contributions from both downwelling solar spectral radiance (i.e., direct solar and scattered

downwelling radiance) and downwelling thermal emission; ρ is the reflectance of the associated objects; τ is the atmospherical transmittance; $L_{\text{adj}}(\rho_{\text{adj}})$ is the radiance contributed by adjacent surroundings; L_U is the upwelling radiance.

The mean value of the at-sensor radiance can be expressed as

$$\overline{L}_{AS} = L_D\,\overline{\rho}\,\tau + \overline{L_B(T)}[1-\overline{\rho}]\tau + L_{\text{adj}}\left(\overline{\rho}_{\text{adj}}\right) + L_U \quad (16)$$

assuming ρ and T are statistically independent. This is a reasonable assumption given complex external influences (local radiation environment, wind and solar loading history, etc.) that are specific to a given situation and beyond the scope of our analytical model [9]. The general expression to calculate variance from expectation is

$$\text{Var}(X) = \sigma^2 = \text{E}[(X - \text{E}(X))^2]. \quad (17)$$

Thus, the variance of our at-sensor radiance (σ^2_{LAS}) is

$$\sigma^2_{\text{LAS}} = \tau^2\left[\sigma^2_{LB}\sigma^2_\rho + \overline{L_B}\sigma^2_\rho + \sigma^2_{LB}\left(1-\overline{\rho}\right)^2 + L^2_D\sigma^2_\rho - 2L_D\overline{L_B}\sigma^2_\rho\right] + \sigma^2_{L_{\text{adj}}}. \quad (18)$$

The previous analysis addressed the variance of the at-sensor radiance in a univariate sense. We now examine the multivariate problem, which is related to our work. Assuming there are k-spectral bands for input data, the covariance of at-sensor radiance will be $k\times k$. The covariance of the at-sensor radiance can be written as

$$\begin{aligned}\Sigma_{\text{At-Sensor}} = \Gamma\Big[&\Lambda_{\sigma LB}\Sigma_\rho\Lambda_{\sigma LB} + \Lambda_{\overline{L}B}\Sigma_\rho\Lambda_{\overline{L}B} \\ &+\Lambda_{1-\overline{\rho}}\Sigma_{LB}\Lambda_{1-\overline{\rho}} + \Lambda_{LD}\Sigma_\rho\Lambda_{LD} \\ &-\left(\Lambda_{LD}\Sigma_\rho\Lambda_{\overline{L}B} + \Lambda_{\overline{L}B}\Sigma_\rho\Lambda_{LD}\right)\Big]\Gamma \\ &+\left(\Lambda_{L1_{\text{adj}}} - \Lambda_{L0_{\text{adj}}}\right)\Sigma_{\rho_{\text{adj}}}\left(\Lambda_{L1_{\text{adj}}} - \Lambda_{L0_{\text{adj}}}\right)\end{aligned} \quad (19)$$

where Γ is a diagonal matrix of atmospheric transmittance, $\Lambda_{\sigma LB}$ is a diagonal matrix of standard deviations of blackbody emissions, Σ_ρ is a covariance matrix of the objects' surface reflectance, and $\Lambda_{\overline{L}B}$ is a diagonal matrix of blackbody emissions at a given mean temperature $\overline{T}$. Σ_{LB} is a covariance matrix of blackbody emissions, which can be calculated by $\Lambda_{\sigma LB}[1]\Lambda_{\sigma LB}$, where [1] is a $k \times k$ matrix of ones (here we assume in Σ_{LB} each channel is independent.). Recalling Kirchoff's law, $\epsilon + \rho = 1$, therefore $\Lambda_{1-\overline{\rho}}$ can be treated as a diagonal matrix of emissivities, Λ_{LD} is a diagonal matrix of downwelling spectral radiances, and $\Lambda_{L0_{\text{adj}}}$ and $\Lambda_{L1_{\text{adj}}}$ are the diagonal radiance matrices with surface albedos of 0 and 1, respectively.

Thus, the surface reflectance mean and covariance are in turn propagated through the atmosphere and re-expressed as the at-sensor radiance mean and covariance, as stated in (16) and (19), respectively.

Appendix B
Calculation of the Variance of Y

To solve (12), recall that Variance $= \sigma^2$. Knowing this, one can calculate the standard deviation of Y instead. Using analytical error propagation for a nonlinear function $y = F(x)$, the standard deviation σ_y approximately equals $\sigma_x dF/dx$ where σ_x is the standard deviation of the variable x. Since the only random variable in Y is the blackbody radiance, the standard deviation of Y can be written as

$$\sigma_Y \approx \sigma_{LB}\frac{dY}{dL_B}. \quad (20)$$

Since L_B is a function of the random variable $\hat{T}$, replacing σ_{LB} by a function of $\sigma_{\hat{T}}$, where $\sigma_{\hat{T}}$ is the standard deviation of retrieved temperatures, σ_{LB} can be expressed as

$$\sigma_{LB} \approx \sigma_{\hat{T}}\frac{dL_B}{d\hat{T}}. \quad (21)$$

In our previous research, $\sigma_{\hat{T}}$ can be treated as an user-defined parameter as described in [10] (i.e., $\sigma_{\hat{T}} = 0.1$). Substituting (21) into (20) results in

$$\sigma_Y \approx \sigma_{\hat{T}}\frac{dL_B}{d\hat{T}}\frac{dY}{dL_B} \quad (22)$$

where

$$\frac{dL_B}{d\hat{T}} = L_B c_2\frac{e^{\frac{c_2}{\lambda\hat{T}}}}{\lambda T^2\left(e^{\frac{c_2}{\lambda\hat{T}}} - 1\right)}. \quad (23)$$

Recalling the general derivative relationship, $(1/u') = -(u'/u^2)$. Knowing this, we have

$$\frac{dY}{dL_B} = \frac{\partial\left(\frac{1}{\tau L_B - \tau L_D}\right)}{\partial L_B} = -\frac{1}{\tau(L_B - L_D)^2}. \quad (24)$$

The change of Y is then written as

$$\sigma_Y \approx -\sigma_{\hat{T}}\frac{dL_B}{d\hat{T}}\frac{1}{\tau(L_B - L_D)^2}. \quad (25)$$

Finally, the variance of Y is computed by squaring the standard deviation as σ^2_Y.

References

[1] J. P. Kerekes and D. A. Landgrebe, "An analytical model of Earth-observational remote sensing systems," *IEEE Trans. Syst., Man, Cybern.*, vol. 21, no. 1, pp. 125–133, Jan./Feb. 1991.

[2] J. P. Kerekes, "Parameter impacts on hyperspectral remote sensing system performance," *Proc. SPIE*, vol. 2821, pp. 195–201, Nov. 1996.

[3] J. P. Kerekes and J. E. Baum, "Spectral imaging system analytical model for subpixel object detection," *IEEE Trans. Geosci. Remote Sens.*, vol. 40, no. 5, pp. 1088–1101, May 2002.

[4] C. C. Borel, "Iterative retrieval of surface emissivity and temperature for a hyperspectral sensor," Los Alamos Nat. Lab., NM, USA, Tech. Rep. LA-UR-97-3012, 1997.

[5] C. C. Borel, "Surface emissivity and temperature retrieval for a hyperspectral sensor," in *Proc. IEEE Int. Geosci. Remote Sens. Symp.*, vol. 1, Jul. 1998, pp. 546–549.

[6] C. C. Borel, "ARTEMISS—An algorithm to retrieve temperature and emissivity from hyper-spectral thermal image data," in *Proc. 28th Annu. GOMACTTech Conf.*, Mar. 2003, pp. 1–4.

[7] P. M. Ingram and A. H. Muse, "Sensitivity of iterative spectrally smooth temperature/emissivity separation to algorithmic assumptions and measurement noise," *IEEE Trans. Geosci. Remote Sens.*, vol. 39, no. 10, pp. 2158–2167, Oct. 2001.

[8] M. F. McCabe, L. K. Balick, J. Theiler, A. R. Gillespie, and A. Mushkin, "Linear mixing in thermal infrared temperature retrieval," *Int. J. Remote Sens.*, vol. 29, nos. 17–18, pp. 5047–5061, Sep. 2008.

[9] J. P. Kerekes and J. E. Baum, "Full-spectrum spectral imaging system analytical model," *IEEE Trans. Geosci. Remote Sens.*, vol. 43, no. 3, pp. 571–580, Mar. 2005.

[10] R. Zhao and E. J. Ientilucci, "Improvements to an Earth observing statistical performance model with applications to LWIR spectral variability," *Proc. SPIE*, vol. 10198, May 2017, Art. no. 101980N.